Synthesis of Passive Human Radio Frequency Signatures via Generative Adversarial Network

Jenny Liu
Dept. Elect & Comp Eng
Oakland University
Rochester, MI 48309
Jennyliu443@gmail.com

Robert Ewing
Air Force Research Lab
WPAFB, OH 45433
robert.ewing.2@us.af.mil

Erik Blasch
Air Force Research Lab
Rome, NY 13441
erik.blasch.1@us.af.mil

Jia Li
Dept. Elect & Comp Eng
Oakland University
Rochester, MI 48309
li4@oakland.edu

Abstract—**Human occupancy in an enclosed space can cause variation of the passive radio frequency (RF) spectrum. To assess the RF spectrum variation, a cognitive radio (CR) based human occupancy detection (CRHOD) method successfully determines presence of people. However, a wireless environment can be easily interfered by jamming signals or by replaying recorded samples. Hence, the knowledge of the RF environment is a critical aspect of a passive RF signals-based security monitoring system. Instead of retraining detectors with newly collected data, future systems can adapt to a new environment by predicting the RF signatures with human occupancy given the baseline spectrum of the environment measured without human occupancy. Synthesizing RF signatures of human occupancy is a challenging research area due to the lack of prior knowledge of how a human body alters the RF data. A human RF signatures generation system via conditional generative adversarial networks (GAN) is proposed in this paper to synthesize spectrum with human occupancy using the baseline spectrum at the area of interest. First, the trained *human RF signatures GAN* (HSGAN) model synthesizes passive RF signals with human occupancy via the baseline spectrum without human occupancy collected in the enclosed space. Second, the trained HSGAN model predicts the human RF signatures in the enclosed space at a new location using the HSGAN model trained in other locations. Lastly, the HSGAN model is quantitatively evaluated via two classifiers including a convolutional neural network (CNN) model and a k-nearest neighbors (KNN) classifier for the quality of the synthesized spectrum. In addition, a 99.5% correlation between synthesize human RF signatures and real human RF signatures results from the HSGAN.**

Table of Contents

978-1-7281-7436-5/21/$31.00 ©2021 IEEE

1. Introduction

Human occupancy detection (HOD) has been applied in many field including smart building monitoring [1], autonomous vehicle passenger inspection [2], human tracking motion analysis [3] and robotic system safety [4]. Different technologies have been applied to solve the HOD problem using various sensing modalities such as visual cameras [5] and thermal imagers [6], lidar [7] and radar [8], [9] infrared [10], and ultrasonic [11] sensors. All these technologies have individual advantages and weaknesses. For example, visual cameras are restricted by lighting although they can provide images which can be applied to human subject identification and tracking. Furthermore, cameras can be invasive thus they are limited when privacy is a concern. Signal emitters are the essential parts of lidar and radar systems. The actively emitted signals can interfere with existing wireless systems and are not environment friendly. Other detectors such as infrared, ultrasonic and all the modalities mentioned above are constrained by the installation angle and position. Therefore, a passive, non-polluting, and low-priced sensing solution is beneficial for HOD.

By analyzing passive RF signals variation caused by human anatomy, a cognitive radio (CR) based human occupancy detection (CRHOD) system successfully detects the presence of people in the enclosed spaces [12]. However, adversaries can easily jam a wireless environment by emitting interference RF signals or simply replaying the recorded data. A passive RF signals-based security monitoring system should have the awareness of the RF environment to maintain its reliability and robustness. RF environments vary with locations. Thus, the system should easily adapt to a new environment with minimum user effort through synthesis of human RF signatures after measuring the baseline spectrum of the new environment. The knowledge of spectrum variation caused by human occupancy and synthesizing human RF signatures are critical aspects of building a more efficient, robust, and secure real-time indoor monitoring system. An open question this paper addresses is whether this variation can be synthesized.

Generative adversarial networks (GAN) are powerful tools which can learn from labeled samples and generate features

2021 IEEE Aerospace Conference | 978-1-7281-7436-5/21/$31.00 ©2021 IEEE | DOI: 10.1109/AERO50100.2021.9438476

based on the knowledge gained. GANs have been widely used in areas such as synthesizing artificial images, text articles, human voices, and wireless signatures [13]–[20]. GANs are usually built with two neural networks, a generator and a discriminator, competing with each other in order to discriminate which data imitates the real data. The generator produces faked data to fool the discriminator and the discriminator distinguishes between the synthetic and the real instances of data. Both models become more robust during the competition.

A human RF signatures generation system via conditional GAN is proposed in this paper to synthesize RF signals through the baseline spectrum at the area of interest. A low-cost software defined radio (SDR) scans the spectrum from its lowest frequency to its highest frequency in an enclosed space with and without human occupancy. Labels are automatically assigned to the collected samples. The GAN generator is fed with the average power of frequency bands in the collected baseline spectrum and generates the average powers to simulate the spectrum with human occupancy. The GAN discriminator discerns the generated spectrum from the real spectrum with human occupancy through classification. The errors of classification results are backpropagated to train the generator to maximize the classification errors and to train the discriminator to minimize the classification errors. The process repeats to optimize the performance of both models.

To the best of our knowledge, it is the first time that a GAN is used to generate passive human RF signatures in the application of HOD. The main contributions of this paper are: (1) a *human signatures GAN* (HSGAN) model is proposed to synthesize passive RF data in the enclosed space and the proposed HSGAN model can generate human RF signatures via a baseline spectrum; (2) the trained HSGAN model can predict the human RF signatures in a new environment via transfer learning where the variation of wireless signals caused by human body are unseen during training; (3) the synthesized RF data is quantitatively evaluated by the HOD results and calculated correlation between the generated signals and real signals; (4) the comprehensive measured results are presented in this paper for operational usability.

The rest of the paper is as follows. Section 2 introduces related research works and comparisons to the HSGAN solution. Section 3 explains applied technologies and the detailed experimental design. The experimental results are presented in Section 4. Conclusions and future research are discussed in Section 5.

2. BACKGROUND

2.1. Related work

2.1.1. Human Occupancy Detection

Human occupancy detection (HOD) is sometimes referred to as occupancy detection. Different technologies have been utilized for HOD including analysis of wireless RF signals and video surveillance. The development of wireless technologies increased attention for HOD such as infrared, RFID, and Wi-Fi network sensing, sparse vibration sensors and active RF signals assessed in [1], [10], [21]–[23]. However, all the solutions mentioned above either depended on certain types wireless signals, required significant installations, or emitted active wireless signals. Edrich et al. [24] proposed to detect objects through passive RF data in the application of airspace surveillance, but HOD was not within their published research. Cameras were used for HOD inside a vehicle by Birch et al. [2] and in a building by Shih et al. yet visual images were not desirable when privacy was favorable [25]. Passive CR was utilized by [12] to collect passive RF data and applied to HOD through data analysis which compensated for the solutions mentioned above. This method did not relay on specific types of wireless signals and/or privacy protection. For example, the low cost and environmentally friendly solution did not emit active signals nor occupy the crowded communication channels. Furthermore, it was easy to deploy the detection devices and to adapt a new environment. Current methods can take advantage of simulated data for training [26].

2.1.2. Generative Adversarial Networks

The wireless environment is difficult to control and is vulnerable to jamming signal disturbance sent by malicious devices. Knowing and inspecting the spectrum at the location of interest becomes an indispensable part of HOD from wireless signals. Researchers have initiated various approaches to protect the security of wireless environment. SDR and convolutional neural network (CNN) were used by Riyaz et al. to detect and identify a specific radio transmitter uniquely among other similar devices [27]. The emitter of the wireless signal were classified by four machine learning (ML) algorithms from the adversarial devices by [28] [29]. However, both research works mention passively monitor the wireless environment instead of proactively predicting spectrum variations. Generative models in ML project the changes in the wireless network. The GAN was proposed by J. Goodfellow et al. in 2014 to estimate the generative model via the adversarial process [30]. The GAN has been widely employed in multiple areas and drew attention from some researchers in the field of wireless communication due to its capability of synthesizing data. Roy et al. [31] used the RF data generated by GAN to simulate the spoofing signals thus the rogue transmitters could be recognized from the trusted devices through the classifier which was trained with the simulation data and trusted data. Missing spectral information was recovered via GAN by Tran et al. [32] in domain of a ultra-wideband (UWB) radar system. Li et al. [33] implemented sparsely self-supervised GAN to estimate the corrupted cellular network data. The significant accuracy improvement was made by Liu et al. [34] in the field of real-time smartphone indoor localization via GAN. With these very promising outcomes from the above studies, there is motivation to apply GANs to train a generative model which can predict human RF signatures through the baseline spectrum via the adversarial process.

GAN can be extended to conditional model by providing auxiliary information which it conditions on. Comparing to the original GAN which the generated data is not controlled by the model, the conditional model is capable of directing the data generation process. These additional information can be any type of supplementary data such as the classification labels and output from other sensors. Mirza et al. fed the classification labels along with the random data into both the generator and dissimilator to generate images. Their preliminary experiments demonstrated the potential of conditional GAN and the useful applications [35]. Superior de-raining images were obtained by feeding the adversely affected images captured during raining into the generator of the conditional GAN [36]. The RF ultrasound plane wave channel data was employed as the input signals of the conditional GAN in order to generate high quality B-mode images [37]. Our HSGAN model uses the baseline spectrum as the input of the generator to estimate the actual spectrum with human occupancy.

2.1.3. Cognitive Radio

Cognitive radio (CR) evolved from *software defined radio* (SDR) by adding additional functions such as wireless environment assessment, spectrum changes tracking, parameter reconfiguration, and environment-based reaction. CR emerged in the recent decades due to innumerable wireless devices and rapid deployment as described by Jondral [38]. The fixed channel allocation policy causes inefficient usage of limited spectrum resources. CR is urged by its innovative technology and is applied quickly and widely. The development of a dynamic spectrum access network was enabled by CR through which the spectrum and energy could be utilized more efficiently in an opportunistic fashion [39] and the inference with licensed users could be voided [40]. CR has been employed in the domains such as wireless communication power consumption saving through active channel utilization, intelligent channel allocation, smart grid energy reduction by automatically monitoring and controlling grid activities by incorporating the CR communication network [41]–[44]. Significant power is reduced via CR in the application of HOD using only the significant frequency bands data and the performance can be maintained without using full bands data [12].

CR is utilized in this research to synthesize human RF signatures in order to build a more energy efficient and eco-friendly HOD system. Furthermore, considering that the spectrum is not the same at different locations, CR can help to build more flexible system which can fit new wireless environments easier by sensing its surroundings circumstance. A low cost SDR is configured in our experiment to collect the data at the location of interest and adjusted based on the observed spectrum status.

2.1.4. Feature Selection

Signals, features, and decisions are the three common elements of classification methods. Passive RF based HOD system classifies the human RF signatures from the baseline spectrum that recognizes the space occupancy status. Earlier research works suggested properly selected features cannot only simplify the classification model and reduce the training time, but also enhance the model's generalization [45]–[48]. Our previous study indicates that certain frequency bands are sensitive to HOD, but others are not [12]. Thus, it is not necessary to process all the signals since the same accuracy can be achieved with reduced data size. Moreover, the system efficiency would decrease, and energy would be wasted if all the data in the whole frequency bands supported by the SDR is processed including those not responsive to HOD. So, the insensitive frequency bands data was eliminated from CRHOD system and the system maintained the same reliability [12].

Synthesizing human RF signatures should adopt the same strategy without generating redundant or irrelevant features in the data. A Feature selection algorithm based on the principal component analysis (PCA) is utilized to pick the frequency bands which are sensitive to HOD and only these selected frequency bands data in the baseline spectrum are fed to the HSGAN model. PCA is an unsupervised feature selection algorithm which needs less computation power and does not require the training data to be labeled as compared to supervised feature selection algorithms, e.g. recursive feature elimination with logistic regression (RFE-LR). RFE-LR consumes more calculation power and training samples must be labeled but without notable performance improvement in the application of HOD [12].

2.2. Advantages

This paper proposes a *human RF signatures synthesis* (HSGAN) model which generates the RF signals from the baseline spectrum at the location of interest. A SDR scans the spectrum from its lowest frequency to its highest frequency in an enclosed space with and without human occupancy, where labels are automatically assigned to the collected samples. Frequency bands sensitive to HOD are selected by the PCA algorithm. The HSGAN is trained with the average powers in the selected frequency bands of the baseline spectrum, HSGAN then generates average powers in the same frequency bands to simulate the spectrum with human occupancy. There are several advantages offered by the HSGAN approach. Firstly, through proactively predicting the wireless environment at the location of interest, the passive RF based HOD system is capable of recognizing the spoofing or jamming signals which are used to disturb ambient spectrum from the real human RF signatures. Secondly, the passive RF based HOD system can fit a new spectrum circumstance easier without retaining the classifier. It enhances flexibility of the system and the maintenance coast is reduced. Lastly, through bands selection strategy, only the signals containing important information are synthesized from which the efficiency of the system is increased.

3. METHODOLOGIES

A human RF signatures synthesis system is built in our experiment and is depicted in Figure 1. The system includes a receiving antenna, an SDR, a data reprocessing module, a band selection module, and a HSGAN module.

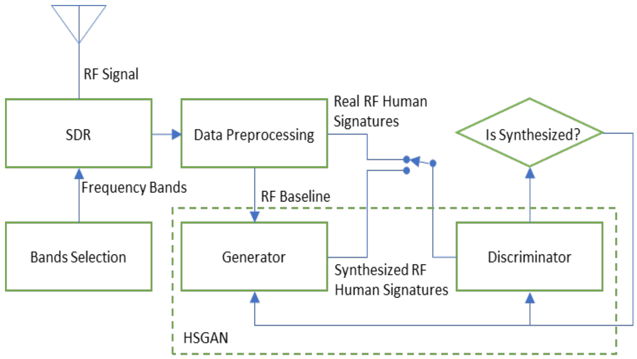

Figure 1. Human RF signatures synthesis system

The RF signals are collected from enclosed spaces. In the initial stage, the SDR is configured to scan the whole spectrum in its frequency range (24-1760 MHz). Meanwhile, the collected data is automatically labeled, and the collected RF signals corresponding to the human occupancy status are associated to the labels. After enough whole spectrum samples are collected, the frequency bands which are sensitive to HOD are selected. Then, only the selected frequency bands are scanned by the reconfigured SDR. The HSGAN including a generator and a discriminator are trained with the baseline spectrum and the human RF signatures in the selected frequency bands. The generator synthesizes the RF human signals to simulate the spectrum when the enclosed space is occupied. Lastly, a CNN model and a k-nearest neighbors **(**KNN) model are trained with the real signals in the selected frequency bands with and without human occupancy at the location of interest.

The performance of human RF signatures synthesis system is evaluated by the classification results of the trained CNN and KNN models taking the inputs of the real baseline spectrum and the synthesized RF data. The signal acquisition and pre-processing are introduced in subsection 3.1 and 3.2. Subsection 3.3 illustrates the frequency bands selection algorithm. Finally, the structure of HSGAN, the training process and evaluation methods are presented in Subsections 3.4, 3.5, and 3.6.

3.1. RF signal Acquisition

Only a laptop, SDR, and cell phone are used to collect data in the enclosed space in order to eliminate the data contamination from irrelevant electronic devices. Regardless of the occupancy status, the laptop and SDR are always in working status. The real-life environment wherein people carry their cell phones in most situations is simulated by leaving the cell phone powered on or off in the enclosed space randomly, regardless of the occupancy status. The cell phone assures the experiment does not depend on the signals emitted by the cell phone. A low-cost SDR, RTL2832U, is used to collect the RF raw data at two separate locations, a study room in a single family house and a fourth floor office in a six floors building, with and without a human subject occupying the enclosed spaces. The labels are automatically

Table 1. SDR configuration of passive RF data collection.

Items	Description
SDR	RTL2832U
Locations	a study room, an office
Data Labels	0: Unoccupied 1: Occupied
Frequency Range	24 MHz–1760 MHz
Scanning Step	1.2 MHz
Bandwidth	1.2 MHz
Sampling Rate	2.4 MHz
Duration	2 ms per frequency band
Number of Frequency Bands	1447

assigned to the RF raw data by the program during wireless signals collection. The spectrum is continuously scanned by the SDR with an even step size of 1.2 MHz from its lowest frequency 24 MHz to its highest frequency 1760 MHz during a full band scan. The passive RF data collection information is described in Table 1.

A *full band sample* refers to the frequency data collected through a scan from the lowest frequency to the highest frequency. One full band sample has 1447 frequency bands. The sampling rate is set at 2.4 MHz. One frequency band is scanned for 2 ms and 4800 samples per frequency band are collected. The verified highest sample rate is 2.4 MHz at which the regular universal serial bus (USB) controllers do not lose samples although the maximal sample rate specified by manufacturer is 3.2 MHz. At each experiment location, the antenna is placed at a fixed position and orientation. Two identical SDRs are used to collect the data which can reduce the data collection time and can eliminate the device dependency. A total number of 1296 full band samples with human occupancy and an equal number of samples without human occupancy were randomly collected in the study room from 6 am to 10 pm across 3 months to eliminate the impact of spectrum variation among different timeframes in the day. 879 full band samples with human occupancy and equal number of samples without human occupancy were collected in the office with the same strategy.

3.2. RF signal Pre-Processing

The average power per frequency band is calculated and is used throughout the experiment. N denotes the number of samples per frequency band which value is 2400. $p(f)$ is the average power of the frequency band centered at f. The value of $p(f)$ is calculated by following equation with the unit of DB:

$$p(f) = 10 * \frac{log_{10}\left(\sum_{i=1}^{N} a_i(f)^2\right)}{\frac{N}{2}} \tag{1}$$

where $a_i(f)$ is the received amplitude of the i -th intermediate frequency signal at the frequency band of f by the SDR.

3.3. Frequency Band Selection

The $p(f)$ in the power spectrum is used to select the bands sensitive to HOD. In this research work, the PCA algorithm with 1447 $p(f)$ as the input features is applied to extract the principal components. Frequency bands according to their values in the extracted components are selected. It is not suggested to directly use the extracted principal components as the features because subsequent spectrum sensing still has to involve all of the frequency bands, since each principal component is a linear combination of all the original frequency bands [49]. According to the measurement variance, the principal components are ranked from high to low by the importance after they are extracted. Then, the first three components are kept. Lastly, k ($k = 784$) frequency bands are selected which have the highest absolute coefficients in the first three components.

3.4. Human Signature Generative Adversarial Networks

A *Generative adversarial network* (GAN) is a framework proposed by Goodfellow et al. [30] which estimates the generative mode via an adversarial process. During the GAN process, two models including a discriminator D and a generator G are trained simultaneously. The data distribution under estimation is captured by the generator G. The generative model G generates fake samples through its captured distribution. The fake samples and real training data are fed to the discriminator D which classifies if the input samples come from the training data rather than generated by G. The training process is a two players' game. The goal of G is to maximize the probability of D to make the mistakes and the goal of D aims to minimize its chances to be fooled by G. In HSGAN, the human RF signatures are synthesized via the baseline spectrum. The discriminator loss $\mathcal{L}_D$ and the generator loss $\mathcal{L}_G$ are defined as follows:

$$\mathcal{L}_D = E_{p_o(f)\sim F_o}\left[\log D\left(p_o(f)\right)\right] + E_{p_u(f)\sim F_u}\left[\log\left(1 - D\left(G\left(p_u(f)\right)\right)\right)\right] \quad (2)$$

$$\mathcal{L}_G = E_{p_u(f)\sim F_u}\left[\log\left(1 - D\left(G\left(p_u(f)\right)\right)\right)\right] \quad (3)$$

The average power for each band of the selected k frequency bands with and without human occupancy are denoted by $p_o(f)$ and $p_u(f)$ respectively. F_o is the probability distribution of $p_o(f)$ and F_u is the probability distribution of $p_u(f)$. G estimates the human RF signatures probability distribution from the input $p_u(f)$ instead of random data. The training is defined as:

$$\max_D \min_G C(G;D) = \mathcal{L}_D \quad (4)$$

The generated data $G\left(p_u(f)\right)$ from G and real sample $p_o(f)$ are fed to D. D estimates the probability of its input is $G\left(p_u(f)\right)$ rather than $p_o(f)$. The cross-entropy cost function $C(G;D)$ depends on both the generator G and the discriminator D. The calculated loss $\mathcal{L}_D$ is propagated back to update both G and D. G maximizes $\mathcal{L}_D$ and D minimizes $\mathcal{L}_D$. The G is optimal when the D cannot distinguish $G\left(p_u(f)\right)$ from $p_o(f)$. The D is optimal when the D can recognize $p_o(f)$ from generated $G\left(p_u(f)\right)$. The process repeats till both models are optimized.

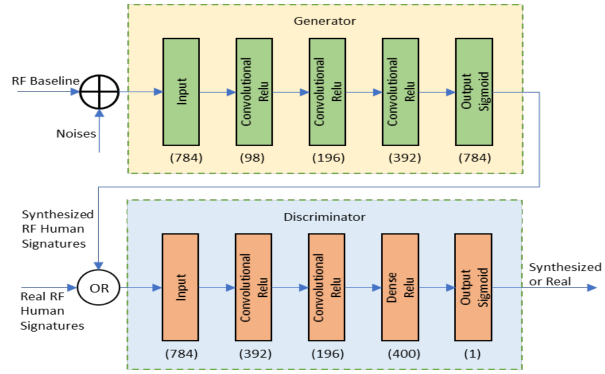

Figure 2. HSGAN structure

Both model G and D are CNNs and their designs are shown in Figure 2. G has 5 layers including one input layer, three convolutional layers and one output layer. The number of neurons and activation functions of each layer are displayed in Figure 2. Similarly, D has 5 layers including one input layer, two convolutional layers, one dense layer and one output layer. The number of neurons and activation functions of each layer are also displayed in the figure.

3.5. HSGAN Model Training

These extracted $p_o(f)$ and $p_u(f)$ from the power spectrum collected are randomly selected as the training and validation samples. These samples are used for HSGAN model fitting and evaluation. Only the samples of the study room are used to train the HSGAN model. The trained HSGAN model generates k average powers to simulate human RF signatures which is donated as $p_{so}(f)$. Each value in the samples is normalized before fitting the model and the normalized data range is from 0 to 1. Uniformly distributed noise ranging from -0.0001 to 0.0001 is added to each value in the training sample in order to improve the model's generalization from which the sample is fed to G. The outputs from generator, of $p_{so}(f)$ and $p_o(f)$ in the training sample, are fed to D alternately. The Adam optimizer is used during training, the learning rate is 0.0002, beta1 is 0.5, beta2 is 0.999 and epsilon is 1e-8. Batch size is 4 and total 90 epochs is trained till both Gand D are optimized.

3.6. HSGAN Model Evaluation

In order to evaluate the performance of HSGAN model, two classifiers including a CNN and a KNN are built to take the input of generated $p_{so}(f)$ and $p_u(f)$ to estimate occupancy status. To build these two classifiers, CNN and KNN models are trained with the real data, $p_u(f)$ and $p_o(f)$ of the study room and corresponding labels, where the number of training samples are 70% of the number of collected samples of each occupancy status, which is 907 out of 1296. The rest 389 samples of each occupancy status are used for testing which are unseen during the training of CNN and KNN. The number of 1296 samples of $p_{so}(f)$ are synthesized by G taking the input of $p_u(f)$ of the study room which is added by uniformly distributed noises ranging from -0.0001 to 0.0001 before being fed to G. Then, the generated 1296 samples of $p_{so}(f)$, including the 389 samples of $p_u(f)$ and corresponding labels, are fed to trained CNN and KNN models for classification. Similarly, the number of 879 $p_{so}(f)$ are synthesized using the data $p_u(f)$ of the office scene are evaluated by CNN and KNN models. These two trained classifiers should be able to accurately distinguish the occupancy status, and the classification results indicate the performance of our proposed HSGAN. Apart from these two classifiers, the correlation between generated data and real data is also calculated for evaluation.

4. Experimental Results

The HOD accuracy of CNN and KNN are used to quantify the overall performance of HSGAN. In order to present the evaluation results of these two classifiers, a confusion matrix is developed. The confusion matrix is determined from the accuracy, precision, recall, and F1 scores from the true positive (TP), true negative (TN), false positive (FP), and false negative (FN) results. The accuracy, precision, recall, and F1 score are determined as:

$$\text{accuracy} = \frac{\text{TF+TN}}{\text{TP+FN+TN+FP}} \tag{5}$$

$$\text{precision} = \frac{\text{TP}}{\text{TP+FP}} \tag{6}$$

$$\text{recall} = \frac{\text{TP}}{\text{TP+FN}} \tag{7}$$

$$\text{F1} = \frac{2\times\text{precision}\times\text{recall}}{\text{precision+recall}} \tag{8}$$

4.1. Synthesized human RF signatures

Figure 3 depicts examples of synthesized human RF signatures and baseline spectrum at the location of study room. Figure 3(a) presents an example of the average powers in the selected 784 frequency bands generated by HSGAN model using baseline spectrum when the study room is unoccupied and Figure 3(b) is a real sample of human signatures collected when the study room is occupied. The overall trends of these two samples are similar and the peaks appear at similar frequency bands such as 0.1 GHz, 0.2 GHz, 0.37 GHz, 0.48 GHz, 0.69 GHz, and so on. The two samples have valleys at similar frequencies as well. A total number of 1296 samples of human RF signatures are generated from 1296 samples of baseline spectrums. To better examine the synthesized signals, the average over all generated human RF signatures, corresponding baseline spectrums, and real human RF signatures are illustrated in Figure 3(c). The red color represents the real signals with human occupancy, the blue line is the baseline spectrum and the gray line is synthesized. The red line and gray line are closer in the gaps in most frequency bands, especially the bands from 0.48 GHz to 1.3 GHz. However, in the lower frequency bands below 0.48 GHz, an opposite relationship is obtained. The synthesized signals are slightly above the real signal with

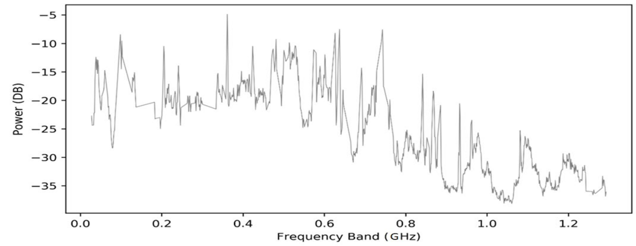

(a) Synthesized

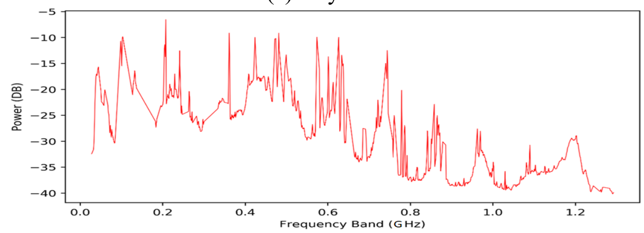

(b) Real

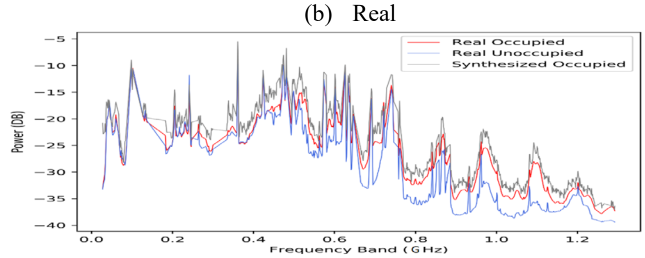

(c) Comparison of the real and synthesized spectrum

Figure 3. Synthesized human RF signatures using data collected in the study room.

human occupancy in the frequency bands higher than 0.17 GHz but almost overlap in the bands lower than 0.17 GHz. Further investigation is needed to study the reasons so that model enhancement can be made.

The correlation between the generated RF data and the real signals with human occupancy, and the correlation between the real signals with human occupancy and without human occupancy are shown in Figure 4. The correlation is calculated using the 1296 generated samples collected with and without human occupancy in the study room. The real occupied signals have a closer relationship with the generated signals as determined by the correlation between the real occupied signals and real unoccupied signals which is consistent with the visual observation.

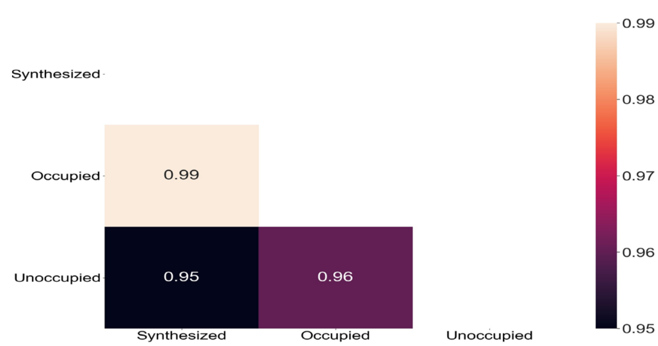

Figure 4. Correlation of synthesized occupied RF data and real data in the study room.

4.2. Evaluation via detection results

Besides visually inspecting the generated signals, and calculating the correlation between the generated data and the real data, the HSGAN is also evaluated by HOD results. The CNN and KNN classifiers are trained with the real collected data with and without human occupancy in the study room. These two trained models take the inputs of synthesized data and baseline spectrum of study room or office, respectively. The detection results of each model at the two locations are listed in Table 2. Both models achieve very encouraging detection performance. The proposed HSGAN can not only generates the human RF signatures at the location of the RF signals in the study room, but can also predict the human RF signatures for a different location using the baseline spectrum at the new location, e.g., the office specifically, as a form of transfer learning or domain adaptation.

Table 2. Detection results of synthesized human RF signatures.

Location	Model	Precision	Recall	F1	Accuracy
Study Room	CNN RNN	100% 98.33%	99.92% 100%	99.96% 99.16%	99.94% 98.69%
Office	CNN RNN	99.77% 98.98%	99.43% 99.66%	99.60% 99.32%	99.39% 98.95%

5. CONCLUSIONS

This paper presents a human RF signatures synthesis system using a conditional GAN. The generated spectrum simulates the wireless signals in an enclosed space occupied by a human subject using the baseline spectrums without human occupancy. The system is based on the GAN model and software defined radio technology. The experimental results show that the proposed HSGAN model is not only capable of synthesizing the human RF signatures using the baseline spectrum at the trained location but also predicting human RF signatures using the baseline signals at a new location without training. The synthesized RF spectrum is evaluated quantitatively by CNN and KNN based classifiers which are trained using the measured spectrum with and without human occupancy in the enclosed space. When fed with synthesized data and measured baseline spectrum, both classifiers produce HOD accuracy above 98 percent.

Different distances between human subject and antenna may cause different variations in the spectrum. We are investigating indoor positioning via passive spectrum monitoring and the research results will be published in the near future.

ACKNOWLEDGEMENTS

This research was supported by AFOSR grant FA9550-18-1-0287.

REFERENCES

[1] H. Zou, Y. Zhou, J. Yang, and C. J. Spanos, "Towards occupant activity driven smart buildings via WiFi-enabled IoT devices and deep learning," *Energy and Buildings*, vol. 177, pp. 12–22, Oct 2018.

[2] P. M. Birch, R. C. D. Young, F. Claret-Tournier, and C. R. Chatwin, "Automated vehicle occupancy monitoring," *Optical Engineering*, vol. 43, no. 8, Aug 2004.

[3] J. Watada and Z. B. Musaand, "Tracking human motions for security system," in *2008 SICE Annual Conference*, Aug 2008, pp. 3344–3349.

[4] W. Shackleford, G. Cheok, T. Hong, K. Saidi, and M. Shneier, "Performance Evaluation of Human Detection Systems for Robot Safety," *Journal of Intelligent & Robotic Systems*, vol. 83, no. 1, pp. 85–103, Jul 2016.

[5] Y. Hou and G. K. H. Pang, "People Counting and Human Detection in a Challenging Situation," *IEEE Transactions on Systems, Man, and Cybernetics - Part A: Systems and Humans*, vol. 41, no. 1, pp. 24–33, Jan 2011.

[6] J. Baek, S. Hong, J. Kim, and E. Kim, "Efficient Pedestrian Detection at Nighttime Using a Thermal Camera," *Sensors (Basel)*, vol. 17, no. 8, Aug 2017.

[7] T. Taipalus and J. Ahtiainen, "Human detection and tracking with knee-high mobile 2D LIDAR," in *2011 IEEE International Conference on Robotics and Biomimetics*, Dec 2011, pp. 1672–1677.

[8] V. Chen, "Detection and analysis of human motion by radar," in *2008 IEEE Radar Conference*, May 2008, pp. 1–4.

[9] S. Chang, N. Mitsumoto, and J. W. Burdick, "An algorithm for UWB radar-based human detection," in *2009 IEEE Radar Conference*, May 2009, pp. 1–6.

[10] H. Kazuhiko, Y. Nobuyuki, and M. Katsuya, "Human occupancy detection method and system for implementing the same," United States Patent EP0716402A1, Dec 1997.

[11] S. Sonia, A. M. Tripathi, R. D. Baruah, and S. B. Nair, "Ultrasonic sensor-based human detector using one-class classifiers," *International Conference on Evolving and Adaptive Intelligent Systems (EAIS)*, Dec 2015.

[12] J. Liu, H. Mu, A. Vakil, R. Ewing, X. Shen, E. Blasch and J. Li, "Human Occupancy Detection via Passive Cognitive Radio," *Sensors (Basel)*, vol. 20, no. 15, Jul 2020.

[13] Y. Cui and W. Wang, "Colorless Video Rendering System via Generative Adversarial Networks," in *IEEE Int'l Conf. on Artificial Intelligence and Computer App. (ICAICA)*, Mar 2019, pp. 464–467.

[14] X. Huang, Y. Li, O. Poursaeed, J. Hopcroft, and S. Belongie, "Stacked Generative Adversarial Networks," in *IEEE Conference on Computer Vision and Pattern Recognition (CVPR),* July 2016, PP. 1866–1875.

[15] J. Ma, W. Yu, P. Liang, C. Li, and J. Jiang,

"FusionGAN: A generative adversarial network for infrared and visible image fusion," *Information Fusion*, vol. 48, pp. 11–26, Aug 2019.

[16] S. Reed, Z. Akata, X. Yan, L. Logeswaran, B. Schiele, and H. Lee, "Generative Adversarial Text to Image Synthesis," in *The 33rd International Conference on Machine Learning*, Jun 2016, vol. 48, pp. 1060–1069.

[17] H. Zhang, T. Xu, H. Li, S. Zhang, X. Wang, X. Huang and D. Metaxas, "StackGAN: Text to Photo-Realistic Image Synthesis with Stacked Generative Adversarial Networks," in *2017 IEEE International Conference on Computer Vision (ICCV)*, 2017, pp. 5908–5916.

[18] J. Gauthier, "Conditional generative adversarial nets for convolutional face generation," *Class Project for Stanford CS231N: Convolutional Neural Networks for Visual Recognition,* Winter semester, 2014.

[19] S. Pascual, A. Bonafonte, and J. Serrà, "SEGAN: Speech Enhancement Generative Adversarial Network," in *Interspeech,* 2017, PP. 3642–3646.

[20] M. Li, O. Li, G. Liu, and C. Zhang, "Generative Adversarial Networks-Based Semi-Supervised Automatic Modulation Recognition for Cognitive Radio Networks," *Sensors (Basel)*, vol. 18, no. 11, Nov 2018.

[21] H. Li, C. Wan, R. C. Shah, A. P. Sample, and S. N. Patel, "IDAct: Towards Unobtrusive Recognition of User Presence and Daily Activities," in *IEEE Int'l Conference on RFID (RFID)*, Apr 2019, pp. 1–8.

[22] S. Pan, A. Bonde, J. Jing, L. Zhang, P. Zhang, and H. Y. Noh, "Building Occupancy Estimation System using sparse ambient vibration monitoring," in *SPIE 9061, Sensors and Smart Structures Technologies for Civil, Mechanical, and Aerospace Systems 2014*, Apr 2014, vol. 9061.

[23] S. Lv, Y. Lu, M. Dong, X. Wang, Y. Dou, and W. Zhuang, "Qualitative Action Recognition by Wireless Radio Signals in Human–Machine Systems," *IEEE Transactions on Human-Machine Systems*, vol. 47, no. 6, Dec 2017.

[24] M. Edrich and A. Schroeder, "Multiband multistatic Passive Radar system for airspace surveillance: A step towards mature PCL implementations," in *2013 International Conference on Radar*, Sep 2013, pp. 218–223.

[25] H.-C. Shih, "A robust occupancy detection and tracking algorithm for the automatic monitoring and commissioning of a building," *Energy and Buildings*, vol. 77, pp. 270–280, Jul 2014.

[26] E. Blasch, G. Seetharaman, and F. Darema, "Dynamic Data Driven Applications Systems (DDDAS) modeling for Automatic Target Recognition," in *Automatic Target Recognition XXIII*, vol. 8744, May 2013, pp.165–174.

[27] S. Riyaz, K. Sankhe, S. Ioannidis, and K. Chowdhury, "Deep Learning Convolutional Neural Networks for Radio Identification," *IEEE Communications Magazine*, vol. 56, no.9, Sep 2018.

[28] K. Youssef, L. Bouchard, K. Haigh, J. Silovsky, B. Thapa, and C. V. Valk, "Machine Learning Approach to RF Transmitter Identification," *IEEE Journal of Radio Frequency Identification*, vol. 56, no.9, pp 197-205, Dec 2018.

[29] D. Roy, T. Mukherjee, M. Chatterjee, E. Blasch, and E. Pasiliao, "RFAL: Adversarial Learning for RF Transmitter Identification and Classification," *IEEE Transactions on Cognitive Communications and Networking*, vol. 6, no. 2, pp. 783–801, Jun 2020.

[30] I. J. Goodfellow, J. Pouget-Abadie, M. Miraz and B Xu, "Generative Adversarial Networks," in *Advances in Neural Information Processing Systems,* 2014, pp. 2672–2680.

[31] D. Roy, T. Mukherjee, M. Chatterjee, and E. Pasiliao, "Detection of Rogue RF Transmitters using Generative Adversarial Nets," in *Wireless Communications and Networking Conf. (WCNC)*, Apr 2019, pp. 1–6.

[32] D. N. Tran, T. D. Tran, and L. Nguyen, "Generative adversarial networks for recovering missing spectral information," in *2018 IEEE Radar Conference (RadarConf18)*, Apr 2018, pp. 1223–1227.

[33] Z. Li, J. Cao, H. Wang, and M. Zhao, "Sparsely Self-Supervised Generative Adversarial Nets for Radio Frequency Estimation," *IEEE J. on Selected Areas in Communications*, vol. 37, no. 11, pp. 2428–2442, 2019.

[34] X. Liu and X. Wang, "Real-Time Indoor Localization for Smartphones Using Tensor-Generative Adversarial Nets," *IEEE Transactions on Neural Networks and Learning Systems*, pp. 1–11, 2020.

[35] M. Mirza and S. Osindero, "Conditional Generative Adversarial Nets," arXiv preprint arXiv:1411.1784 Nov 2014.

[36] H. Zhang, V. Sindagi, and V. M. Patel, "Image De-Raining Using a Conditional Generative Adversarial Network," *IEEE Transactions on Circuits and Systems for Video Technology*, vol. 30, no. 11, pp. 3943–3956, 2020.

[37] Y. Wang, K. Kempski, J. U. Kang, and M. A. L. Bell, "A Conditional Adversarial Network for Single Plane Wave Beamforming," in *2020 IEEE International Ultrasonics Symposium (IUS)*, Sep 2020, pp. 1–4.

[38] F. K. Jondral, "Software-Defined Radio—Basics and Evolution to Cognitive Radio," *EURASIP Journal on Wireless Communications and Networking*, vol. 2005, no. 3, pp. 275–283, Aug 2005.

[39] G. Wang, K. Pham, E. Blasch, T. M. Nguyen, D. Shen and X. Tian "Cognitive radio unified Spectral efficiency and Energy Efficiency trade-off analysis," in *MILCOM 2015 - 2015 IEEE Military Communications Conference*, Oct 2015, pp. 244–249.

[40] B. Wang and K. J. R. Liu, "Advances in cognitive radio networks: A survey," *IEEE Journal of Selected Topics in Signal Processing*, vol. 5, no. 1, pp. 5–23, Feb 2011.

[41] Y. Shi, K. Davaslioglu, Y. Sagduyu, W. Headley, M. Fowler, and G. Green, "Deep Learning for RF Signal Classification in Unknown and Dynamic Spectrum Environments," in *IEEE International Symposium on Dynamic Spectrum Access Networks (DySPAN),* 2019, pp.1–10.

[42] V. K. Tumuluru, P. Wang, and D. Niyato, “Channel Status Prediction for Cognitive Radio Networks,” *Wirel. Commun. Mob. Comput.*, vol. 12, no. pp. 862–874, 10, Jul 2012.

[43] Y. Lin, C. Wang, J. Wang, and Z. Duo, “A Novel Dynamic Spectrum Access Framework Based on Reinforcement Learning for Cognitive Radio Sensor Networks,” *Sensors*, vol. 16, no. 10, pp. 1675–1697, 2016.

[44] R. Ranganathan , R. Qiu, Z. Hu, S. Hou, M. Pazos-Revilla, G. Zheng, Z. Chen, N. Guo and C. Zhou, “Cognitive Radio for Smart Grid: Theory, Algorithms, and Security,” *International Journal of Digital Multimedia Broadcasting*, vol. 2011, Jun 2011.

[45] U. K. Majumder, E. P. Blasch, and D. A. Garren, “Deep Learning for Radar and Communications Automatic Target Recognition”, *Artech House*, 2020.

[46] G. Vanhoy, N. Teku, and T. Bose, “Feature selection for cyclostationary-based signal classification,” in *International Telemetering Conference*, Jan 2017,

[47] X. Wang, Y. Zhang, H. Zhang, X. Wei, and G. Wang, “Identification and authentication for wireless transmission security based on RF-DNA fingerprint,” *EURASIP Journal on Wireless Communications and Networking*, vol. 2019, no. 1, Sep 2019.

[48] C. E. Galván-Tejada, J. P. García-Vázquez, and R. F. Brena, “Magnetic Field Feature Extraction and Selection for Indoor Location Estimation,” in *2013 12th Mexican International Conference on Artificial Intelligence*, Nov 2014, pp.128–132.

[49] G. P. McCabe, “Principal Variables,” *Technometrics*, vol. 26, no. 2, pp. 137-144, May 1984.

BIOGRAPHY

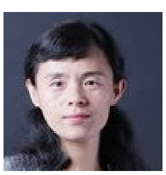

Jenny Liu *is a graduate student in the Department of Electrical and Computer Engineering at School of Engineering & Computer Science of Oakland University. She is studying deep learning neural network-based radio frequency data analysis with Dr. Jia Li. She has 19 years of experience of software engineering and 4 years of experience in artificial intelligence. Her personal research has focused on applications based on deep learning neural network, including stock trading, computer vision, and spectrum monitoring. She is a member of IEEE and is actively involved in technical activities at the school. With her rich project experience, she applies theories and new technologies efficiently in her studies.*

Robert L. Ewing *Dr. Ewing (S'77-M'87-SM-'02-F'14) began his career in the Propulsion Laboratory at Wright-Patterson Air Force Base (Dayton, Ohio) with the development of high-speed jet engine control systems. He later held the position of a medical research scientist at the Aerospace Medical Research Laboratory and Instructor at the Air Force Institute of Technology (AFIT), where he co-pioneered the use of Quantitative Feedback Theory (QFT) for the design of robust analog and digital flight control and aircraft ejection systems. During the early 90's, Dr. Ewing led the Wright Laboratory's Solid State Electronic Devices Directorate's research in the area of mixed-signal hardware description language (VHDL-AMS) for microelectronic VLSI digital design, the IEEE VHDL standards and formal verification of digital designs. He became the Director of the Computer Engineering Research Consortium, a research center composed of universities, industry and graduate students for the innovative development of mixed-signal design methodology & tools, real-time wavelet transforms for video & radar applications, and Spiking Neural Networks for Pattern Recognition. He has authored over 140 journal and conference publications, chaired numerous international IEEE conferences, Adjunct Professor, Associate Editor for Electronic Letters, The Institute of Engineering and Technology (IET) Journal, and Board of Governors, Executive Director, IEEE Aerospace and Electronics Systems Society.*

Erik Blasch *is a program officer with the Air Force Research Laboratory. He received his B.S. in Mech. Eng. from the Massachusetts Institute of Technology and PhD in Electrical Eng. from Wright State University in addition to numerous Master's Degrees in Mech. Eng., Ind. Eng., Elect. Eng., Medicine, Military Studies, Economics, and Business. Additionally, he was a Colonel in the AF reserves, adjunct professor, and president of professional societies. His areas of research include information-fusion performance evaluation, image fusion, and human-machine integration; compiling over 900 papers, 30 patents, and 7 books. He is an Associate Fellow of AIAA, Fellow of SPIE, and Fellow of IEEE.*

Jia Li *received her B.S. degree in electronics and information systems from Peking University, Beijing, China, in 1996, the M.S.E. degree, and the Ph.D. degree both in electrical engineering from the University of Michigan, Ann Arbor, MI, in 1997 and 2002, respectively. She has been a faculty member in the School of Engineering and Computer Science at Oakland University since 2002. Her research interests are in the areas of statistical learning and signal processing with applications in radar, sensor fusion, communications and biomedical imaging. She has authored/co-authored over 70 referred publications, including one book. Her past and current research are sponsored by NSF, NIH, General Motors, Fiat Chrysler, National Research Council, and Air Force Office of Scientific Research. Dr. Li serves as a member of technical committees of several international conferences and workshops. She is a senior member of IEEE.*